187
6-8-81
PH888

(1)

Dr. 2704

HEDL-TME 81-13
UC-79b,h

MASTER

EFFECT OF HEAT TREATMENT UPON THE FATIGUE-CRACK GROWTH BEHAVIOR OF ALLOY 718 WELDMENTS -- PART II, MICROSCOPIC BEHAVIOR

DO NOT MICROFILM
COVER

Hanford Engineering Development Laboratory

HANFORD ENGINEERING DEVELOPMENT LABORATORY
Operated by Westinghouse Hanford Company
P.O. Box 1970 Richland, WA 99352
A Subsidiary of Westinghouse Electric Corporation
Prepared for the U.S. Department of Energy
under Contract No. DE-AC14-76FF02170

DISTRIBUTION OF THIS DOCUMENT IS UNLIMITED

DOE Richland, WA

DISCLAIMER

This report was prepared as an account of work sponsored by an agency of the United States Government. Neither the United States Government nor any agency Thereof, nor any of their employees, makes any warranty, express or implied, or assumes any legal liability or responsibility for the accuracy, completeness, or usefulness of any information, apparatus, product, or process disclosed, or represents that its use would not infringe privately owned rights. Reference herein to any specific commercial product, process, or service by trade name, trademark, manufacturer, or otherwise does not necessarily constitute or imply its endorsement, recommendation, or favoring by the United States Government or any agency thereof. The views and opinions of authors expressed herein do not necessarily state or reflect those of the United States Government or any agency thereof.

DISCLAIMER

Portions of this document may be illegible in electronic image products. Images are produced from the best available original document.

NOTICE

This report was prepared as an account of work sponsored by the United States Government. Neither the United States nor the U.S. Department of Energy (DOE), nor any of its employes, nor any of its contractors, subcontractors or their employes, makes any warranty, expressed or implied, or assumes any legal liability or responsibility for any third party's use or the results of such use of any information, apparatus, product or process disclosed in this report, or represents that its use by such third party would not infringe privately owned rights.

Printed in the United States of America
Available from
DOE Technical Information Center
P.O. Box 62
Oak Ridge, TN 37830

NTIS price codes
Printed Copy: A03
Microfiche copy: A01

HEDL-TME--81-13

DE91 015594

EFFECT OF HEAT TREATMENT UPON THE FATIGUE-CRACK GROWTH BEHAVIOR OF ALLOY 718 WELDMENTS -- PART II, MICROSCOPIC BEHAVIOR

DISCLAIMER

This report was prepared as an account of work sponsored by an agency of the United States Government. Neither the United States Government nor any agency thereof, nor any of their employees, makes any warranty, express or implied, or assumes any legal liability or responsibility for the accuracy, completeness, or usefulness of any information, apparatus, product, or process disclosed, or represents that its use would not infringe privately owned rights. Reference herein to any specific commercial product, process, or service by trade name, trademark, manufacturer, or otherwise does not necessarily constitute or imply its endorsement, recommendation, or favoring by the United States Government or any agency thereof. The views and opinions of authors expressed herein do not necessarily state or reflect those of the United States Government or any agency thereof.

Hanford Engineering Development Laboratory

W.J. Mills
L.A. James

May 1981

DISCLAIMER

This book was prepared as an account of work sponsored by an agency of the Un ted States Government Ne ther the United States Government nor any agency thereof nor any of their employees makes any warranty express or impl ed or assumes any legal l ab lity or respons b l ty for the accuracy completeness or usefulness of any nformation apparatus product or process disclosed or represents that ts use would not infringe pr vately owned rights Reference here n to any spec f c commerc al product process or service by trade name trademark manufacturer or otherwise does not necessarily constitute or imply its endorsement recommendation or favoring by the United States Government or any agency thereof The views and opinions of authors expressed herein do not necessarily state or reflect those of the Un ted States Government or any agency thereof

MASTER

DISTRIBUTION OF THIS DOCUMENT IS UNLIMITED

HANFORD ENGINEERING DEVELOPMENT LABORATORY
Operated by Westinghouse Hanford Company
P.O. Box 1970 Richland, WA 99352
A Subsidiary of Westinghouse Electric Corporation
Prepared for the U.S. Department of Energy
under Contract No. DE-AC14-76FF02170

DISTRIBUTION OF THIS DOCUMENT IS UNLIMITED

HEDL-TME 81-13
UC-79b,h

EFFECT OF HEAT TREATMENT UPON THE FATIGUE-CRACK GROWTH BEHAVIOR OF ALLOY 718 WELDMENTS - PART II: MICROSCOPIC BEHAVIOR

W. J. Mills

L. A. James

ABSTRACT

The microstructural features that influenced the room and elevated temperature fatigue-crack growth behavior of as-welded, conventional heat-treated, and modified heat-treated Alloy 718 GTA weldments were studied. Electron fractographic examination of fatigue fracture surfaces revealed that operative fatigue mechanisms were dependent on microstructure, temperature and stress intensity factor. All specimens exhibited three basic fracture surface appearances at temperatures up to 538°C: crystallographic faceting at low stress intensity range (ΔK) levels, striation formation at intermediate values, and dimples coupled with striations in the highest ΔK regime. At 649°C, the heat-treated welds exhibited extensive intergranular cracking.

Laves and δ particles in the conventional heat-treated material nucleated microvoids ahead of the advancing crack front and caused an overall acceleration in crack growth rates at intermediate and high ΔK levels. The modified heat treatment removed many of these particles from the weld zone, thereby improving its fatigue resistance. The dramatically improved fatigue properties exhibited by the as-welded material was attributed to compressive residual stresses introduced by the welding process.

CONTENTS

		Page
	Abstract	iii
	Figures	vi
I.	INTRODUCTION	1
II.	EXPERIMENTAL PROCEDURE	3
III.	RESULTS	5
	A. MICROSTRUCTURE	5
	B. FRACTURE SURFACE MORPHOLOGY	7
IV.	DISCUSSION	21
V.	CONCLUSIONS	33
VI.	REFERENCES	35

FIGURES

Figure		Page
1	Microstructure of Alloy 718 GTA Weldment	6
2	Electron Fractographs of As-Welded Materials	8
3	Metallographic-Fractographic Profiles at Low Growth Rates	9
4	Metallographic Profile of a Secondary Fatigue Crack at Low Growth Rates in As-Welded Material	10
5	Metallographic-Fractographic Interface in As-Welded Material	12
6	Fractographs of the Conventional Heat-Treated Weld at Low Growth Rates	13
7	Electron Fractographs of the Conventional Weld	14
8	Electron Fractographs of Modified Weld at Low ΔK Levels	16
9	Fracture Surface Morphologies for the Modified Weld	17
10	Typical Fracture Surface Appearance at 649°C	19
11	Comparison of Striation Spacings and Macroscopic Crack Growth Rates at Room Temperature	22
12	Comparison of Striation Spacings and Macroscopic Crack Growth Rates at 538°C	23
13	Typical Longitudinal Residual Stress Distribution in a Weld Compact Specimen and the Resulting Clamping Moment	26
14	Notching of Specimen Blanks	28
15	Front-Face Displacement in the As-Welded Specimen Blank After it was Notched	29
16	Front-Face Displacements in the Specimen Blank that was Annealed at 954°C	30

EFFECT OF HEAT TREATMENT UPON THE FATIGUE-CRACK GROWTH BEHAVIOR OF ALLOY 718 WELDMENTS - PART II: MICROSCOPIC BEHAVIOR

I. INTRODUCTION

In a companion paper,[1] the fatigue behavior of Alloy 718 GTA welds in the as-welded, conventional and modified heat-treated conditions was characterized using linear-elastic fracture mechanics concepts. Crack growth rates in the welds were generally found to be higher than in the wrought superalloy, particularly at the higher stress intensity factor range (ΔK) levels. The fatigue behavior for the two heat-treated welds was similar at low values of ΔK, but at the higher ΔK levels the conventional heat treatment resulted in somewhat higher crack growth rates. The as-welded material exhibited a dramatic improvement in fatigue resistance under low ΔK conditions. At the higher ΔK values, however, crack growth rates in the as-welded material approached those for the heat-treated welds.

Alloy 718 welds are metallurgically complex and involve precipitation of several metastable phases. As a result, the different microstructures resulting from the heat treatments could account for the differences in macroscopic fatigue behavior reported in Reference 1. This portion of the investigation was undertaken to characterize the microstructure and fatigue fracture surface morphology of the welds and to relate heat-treatment variations in crack growth rates to operative fatigue mechanisms and key microstructural features.

II. EXPERIMENTAL PROCEDURE

Light microscopy techniques were used to characterize the microstructures of the Alloy 718 GTA weldments in the as-welded, conventional, and modified conditions.* Metallographic specimens were prepared by standard metallographic procedures and electrolytically etched in an oxalic acid solution to reveal the general microstructure.

Fracture surface micromorphologies for the GTA weldments were characterized by fractographic examination of appropriate test specimens on both transmission and scanning electron microscopes. Standard two-stage carbon replicas, shadowed parallel to the crack growth direction, were prepared from appropriate fracture surfaces for TEM examination. These replicas were cut into small strips approximately 2 to 3 mm wide. Extreme care was taken in measuring the distance from the crack origin to each strip in an effort to relate the features found on the fracture surface to a corresponding growth rate and ΔK level.

To relate fracture surface appearance to key microstructural features, selected areas of the fracture surfaces were electropolished such that the fracture surface topography and underlying microstructure could be studied simultaneously.[2] This technique utilized a protective lacquer applied to portions of the fracture surface that were to remain intact during electropolishing. Exposed surfaces were electropolished in the following electrolyte: 25-gr CrO_3, 7-ml water and 130-ml acetic acid. When electropolishing was complete, specimens were cleaned ultrasonically in acetone to remove the protective lacquer from the unexposed fracture surface. Examination of the interfacial region between the original fracture surface and the electropolished region revealed both the fracture surface topography and the underlying microstructural features.

---

*See Reference 1 for heat-treatments, weld identifications, monotonic and cyclic properties, and chemical composition.

DO NOT MICROFILM
THIS PAGE

III. RESULTS

A. MICROSTRUCTURE

The microstructure of the as-welded Alloy 718 weld zone, shown in Figure 1a, reveals the presence of a white phase in the interdendritic regions, identified by its shape and color as Laves phase. Formation of this topologically close-packed (TCP) phase occurs during the solidification process in microsegregated regions enriched in Nb content. These Laves particles tend to act as localized crack initiation sites, and are believed to be responsible for the low ductility and impact toughness properties exhibited by heat-treated Alloy 718 weldments and castings.[3-5] In the as-welded condition, however, the fracture-resistant matrix arrested microcracks initiated by the Laves phase, and resulted in high ductility and toughness levels.[6]

The typical microstructure of conventional Alloy 718 weldments (Figure 1b) exhibited a significant amount of blocky Laves phase in the interdendritic regions. The inability of the conventional 954°C postweld solution anneal to homogenize the dendritic structure in the weld zone was expected; in previous investigations,[3,7-9] temperatures in excess of 1038°C were required to dissolve the Laves phase. The dark regions surrounding the Nb-rich Laves phase consisted of needle-like δ precipitates, an ordered orthorhombic Ni_3Nb phase, which formed during the 954°C solution anneal. The nucleation of δ needles from Laves particles is also consistent with previous observations in Alloy 718 castings, where the Nb-rich TCP phase acted as a source for δ precipitation.[4,5,10]

The modified heat treatment with a 1093°C solution anneal drastically reduced the amount of Laves phase in the weld microstructure (Figure 1c), which is consistent with observations made at the Idaho National Engineering Laboratory.[8,9] The higher temperature anneal resulted in partial dissolution of the Laves phase, since only relatively small particles remained within the weld zone following the modified treatment.

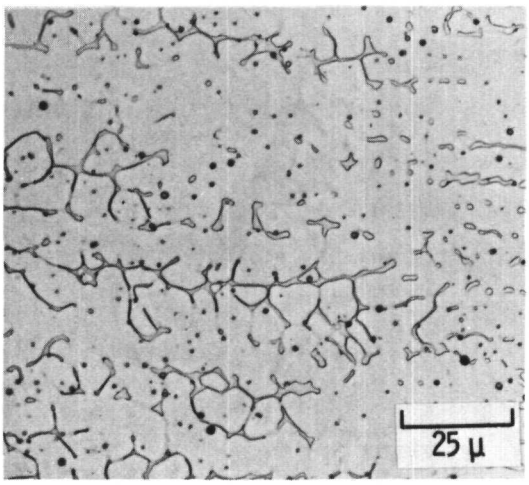

(a)

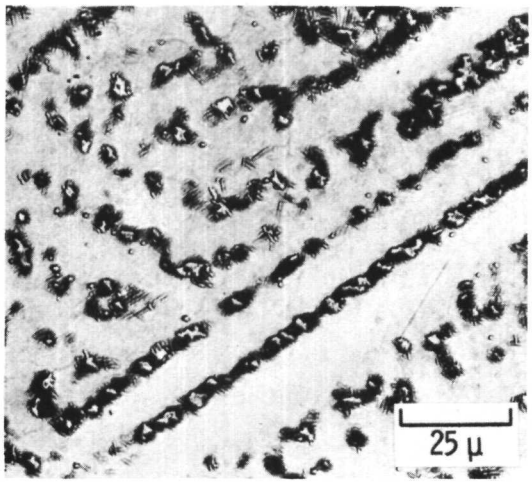

(b)

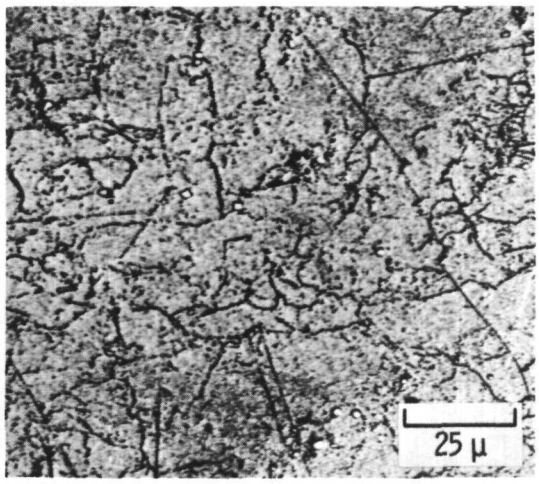

(c)

FIGURE 1. Microstructure of Alloy 718 GTA Weldment.
(a) As-Welded.
(b) Conventional Heat Treatment.
(c) Modified Heat Treatment.

(Neg. 8005394-3)

B. FRACTURE SURFACE MORPHOLOGY

Typical fracture surfaces in the as-welded material tested at temperatures up to and including 538°C exhibited three basic fatigue markings (Figure 2): a faceted or cleavage-like appearance, striations, and dimples. Operative fatigue mechanisms were found to be dependent on the prevailing stress intensity factor, but relatively independent of test temperature. At ΔK levels below 35 $MPa\sqrt{m}$, fracture surfaces took on a cleavage-like appearance (Figure 2a), associated with crystallographic fracture along planar deformation bands. Superimposed on these facets were a series of parallel markings that are believed to be slip offsets. Similar fracture surface morphologies were reported in Alloy 718 base metal.[11]

There is a conspicuous absence of Laves particles on the crystallographic facets (Figure 2a), even though particle density in the underlying microstructure is very high, as indicated by the metallographic-fractographic interfacial region shown in Figure 3a. Figure 4 illustrates the tendency for cracks to avoid the second phase, which accounts for the facets being devoid of Laves particles. The tendency for the fatigue crack to circumnavigate the Laves phase suggests that the overall crack growth behavior at low growth rates is controlled by the fatigue resistance of the matrix. The presence of Laves particles does not appear to influence crack growth rates at low ΔK levels.

Occasionally, fatigue cracks intersected a few Laves particles, and the resulting fracture surface appearance is shown in Figure 2b. The precipitates fractured, but they did not initiate dimples. Apparently local stresses ahead of the crack were high enough to fracture the brittle second phase, but insufficient to cause growth of microvoids. Figure 2b also reveals that the crystallographic facets terminate and subsequently must reinitiate when the advancing crack intersects the Laves particles. Perhaps the additional energy required to reinitiate facets causes the overall tendency for the fatigue crack to avoid these particles.

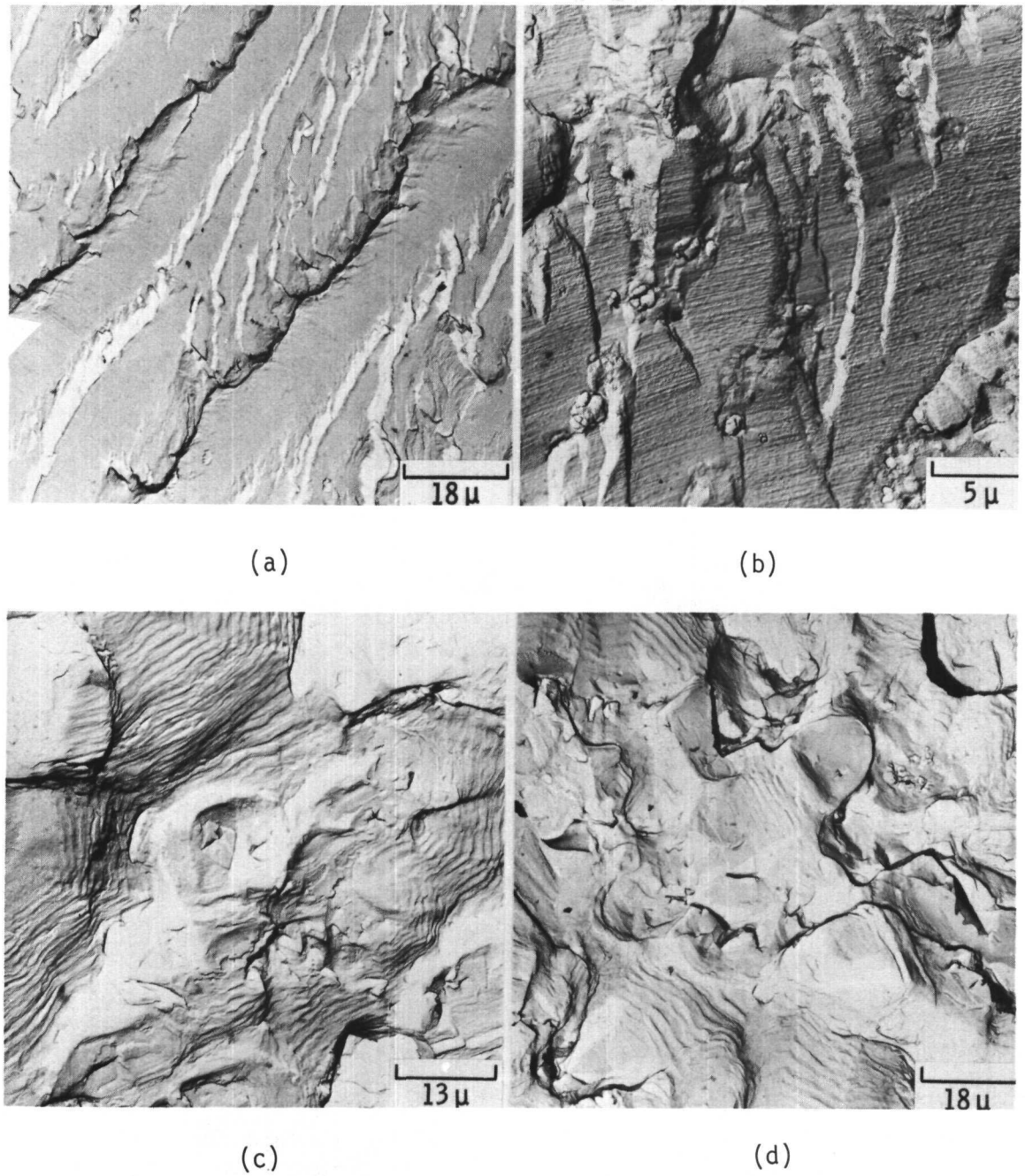

FIGURE 2. Electron Fractographs of As-Welded Materials.
(a) Slip Offsets Superimposed on Crystallographic Facets.
(b) Termination of Facets at Laves Particles.
(c) Rows of Dimples and W-Shaped Striations.
(d) Dimples and Fatigue Striations.

(Neg. 8102955-2)

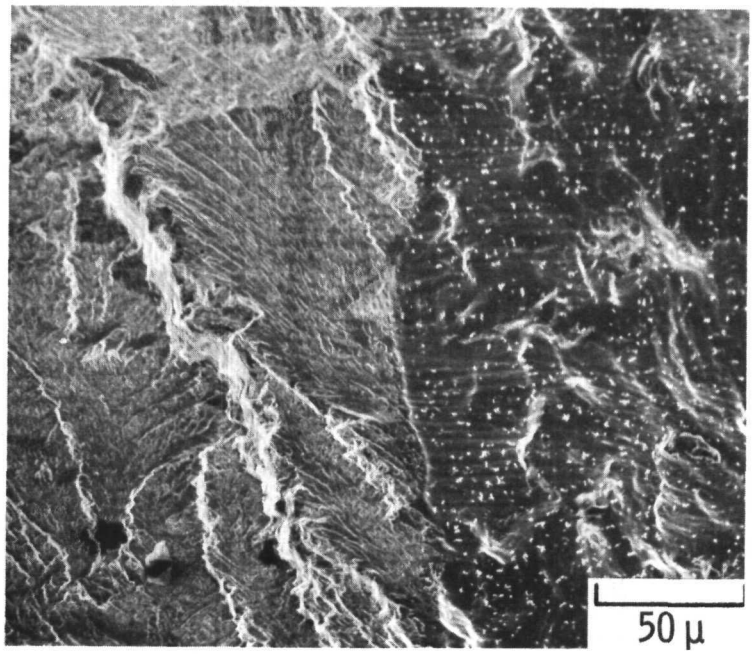

(a)

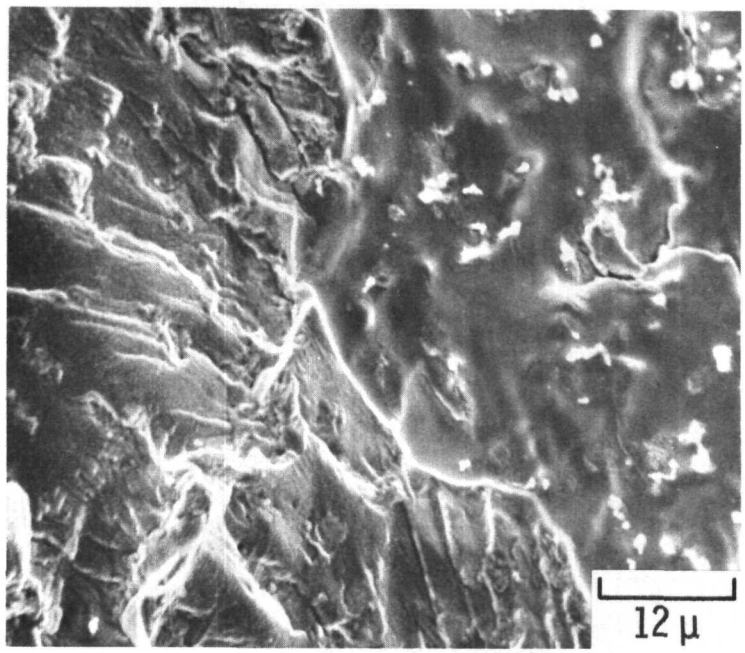

(b)

FIGURE 3. Metallographic-Fractographic Profiles at Low Growth Rates.
(a) As-Welded Condition.
(b) Conventional Condition.

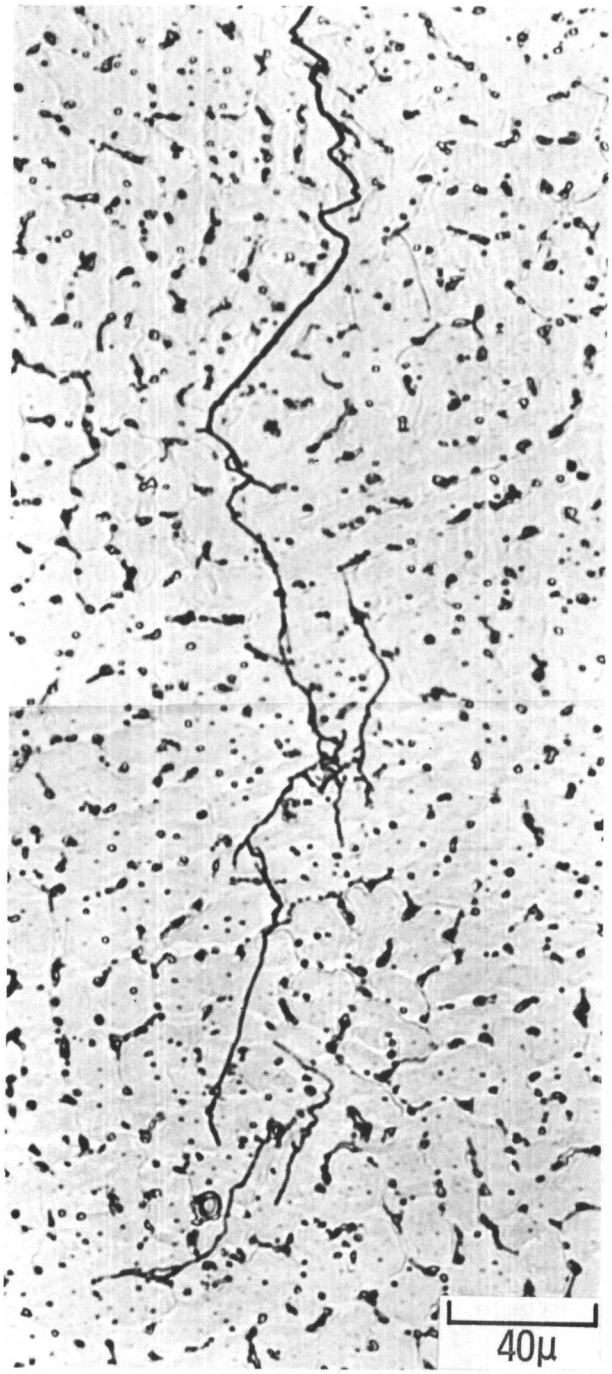

FIGURE 4. Metallographic Profile of a Secondary Fatigue Crack at Low Growth Rates in As-Welded Material.

At intermediate growth rate (5×10^{-5} to 1×10^{-3} mm/cycle), the fracture surface was stratified into consecutive rows of dimples and striations, shown in Figure 2c. The dimples were initiated by Laves particles aligned along the interdendritic regions of the fusion zone. This is illustrated in the metallographic-fractographic interface in Figure 5, where the rows of precipitates in the underlying microstructure (upper region) are aligned with the dimples on the fracture surface. Under the higher ΔK levels, the local stresses are sufficient to cause microvoid coalescence ahead of the advancing fatigue crack. The regions between the rows of dimples are then linked together by striation formation. It is seen that the shape of the striations conforms to the microvoid contours from which they eminate, thereby resulting in the W-shaped striations shown in Figure 2c. At crack growth rates above 10^{-3} mm/cycle, dimples dominated the fracture surface (Figure 2d), and striation formation was confirmed to the small regions between the microvoids.

The conventional heat-treated welds exhibited fracture surface morphologies very similar to those in the as-welded material. At growth rates below 5×10^{-5} mm/cycle, slip offsets were superimposed on the crystallographic facets, as shown in Figure 6a. The straightness and regularity of the slip offsets is displayed in Figure 6b. Relatively few second phase particles were observed on the fracture surface, here again indicating that the fatigue resistance of the weld matrix controls the overall cyclic response at low ΔK levels.

Under slightly higher ΔK conditions, approximately 20 to 25 MPa$\sqrt{m}$, a fracture mechanism transition from faceted growth to striation formation occurred. The faceted appearance became rather nondescript, suggesting that plastic deformation was no longer confined to narrow bands of slip planes, and evidence of Laves and δ precipitates on the fracture surface became more abundant. The higher ΔK levels coupled with the transition from planar slip to wavy slip increased the local strains imposed on the second phase particles causing them to fail and subsequently interact with the advancing crack front. In Figure 7a, the aligned interdendritic precipitates are

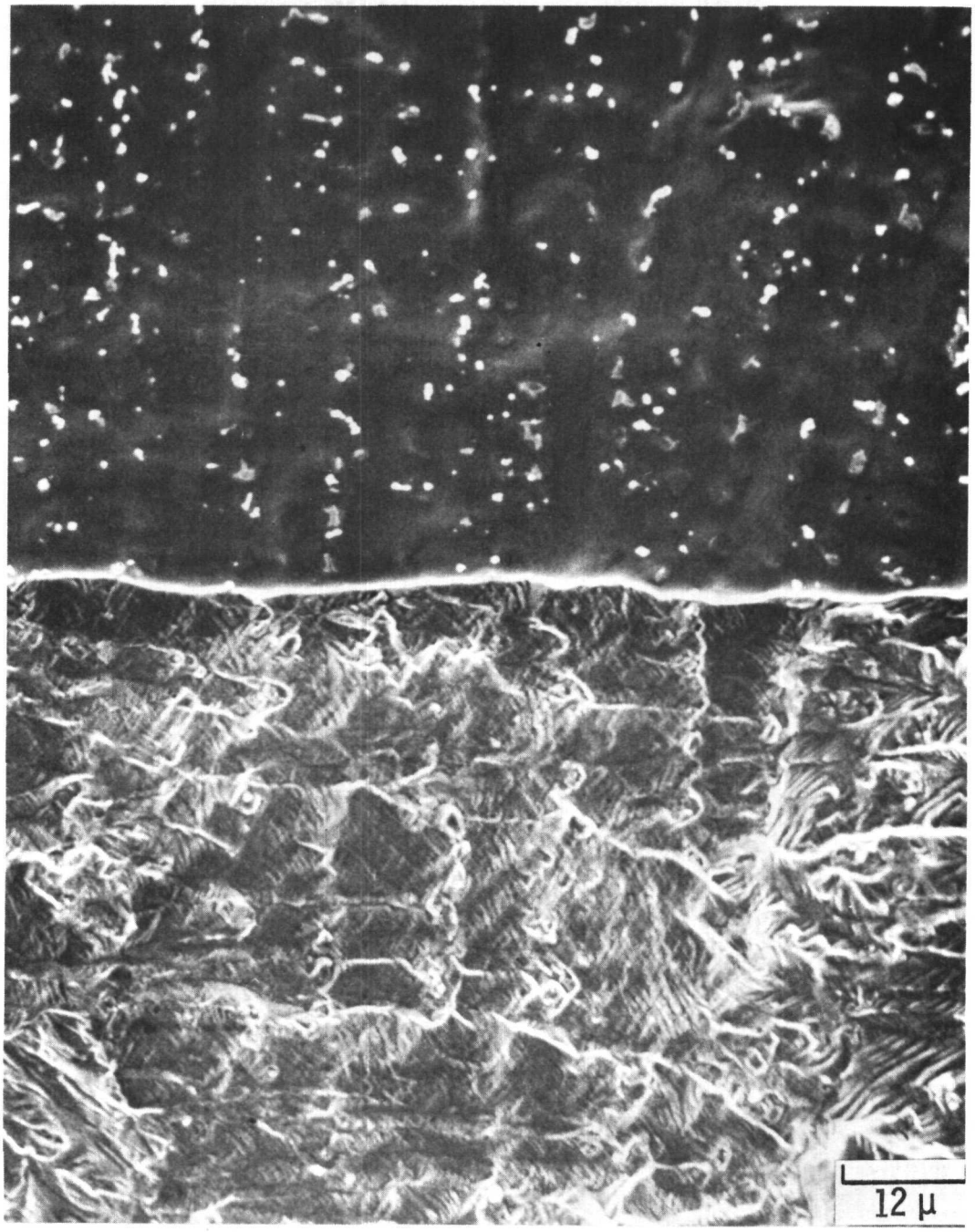

FIGURE 5. Metallographic-Fractographic Interface in As-Welded Material. Rows of Laves Particles in the Underlying Microstructure Aligned with Dimples on the Fracture. Note the W-Shaped Striations in the Background.

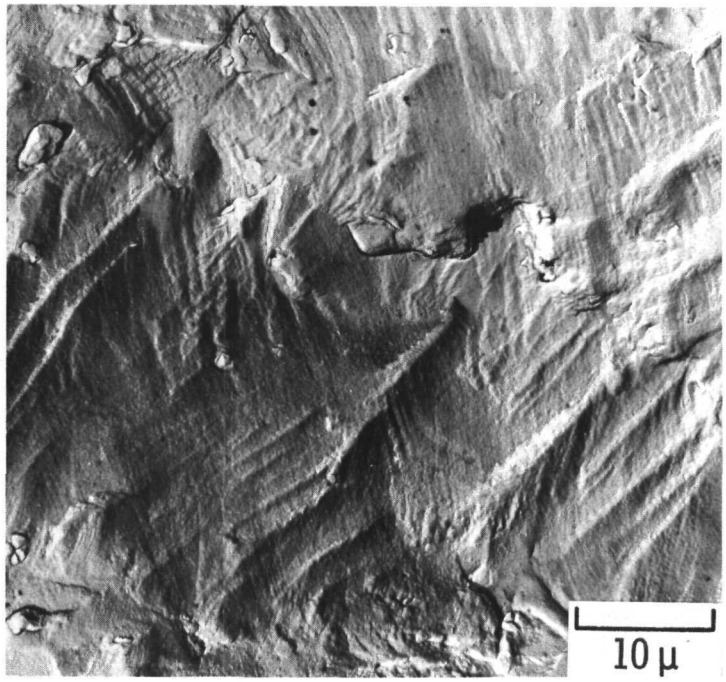

(a)

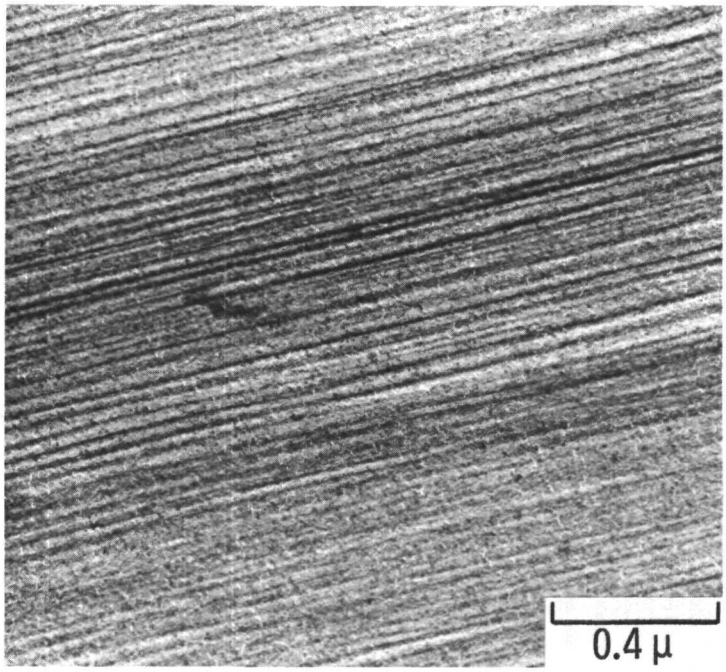

(b)

FIGURE 6. Fractographs of the Conventional Heat-Treated Weld at Low Growth Rates.
(a) Faceted Growth Mechanism.
(b) Slip Offsets.

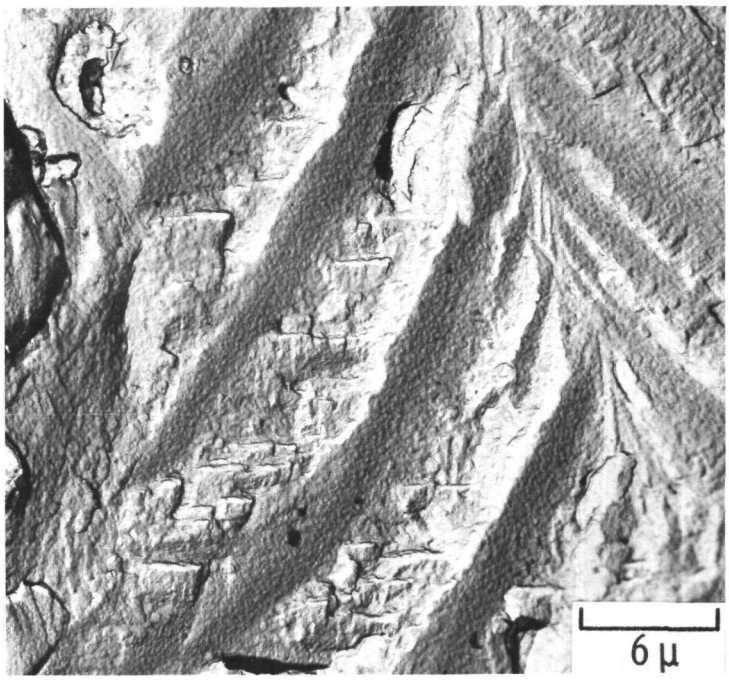

(a)

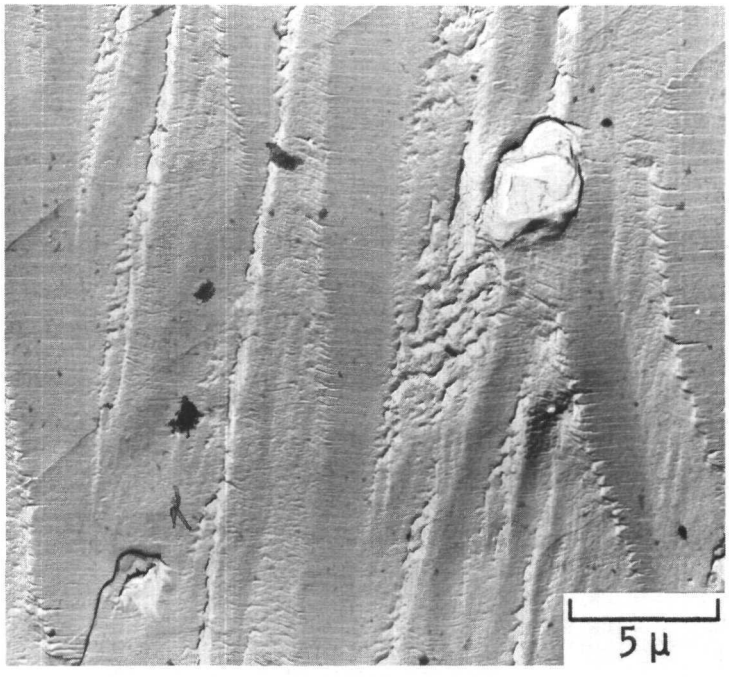

(b)

FIGURE 8. Electron Fractographs of Modified Weld at Low ΔK Levels.
(a) Crystallographic Facets.
(b) Slip Offsets on Facets.

seen to initiate rows of dimples. The regions between the dimples exhibited fine striations and coarse fatigue fissures,[12] generally associated with small secondary cracks emanating from striations. In many regions, the overall shape of the microvoids caused formation of the W-shaped fissures and striations shown in Figure 7b.

At progressively higher ΔK levels (25 to 35 MPa$\sqrt{m}$), the fracture surface consisted of alternating rows of dimples and well-defined striations (Figure 7c). In the conventional weld, individual dimples were much smaller and rather poorly defined in comparison to the as-welded material. Formation of the small, ill-defined dimples was attributed to the many microvoid nucleation sites provided by the Laves and δ precipitates coupled with the high-strength matrix that suppressed plastic deformation around the failed interdendritic particles. At ΔK levels above 35 MPa$\sqrt{m}$, additional evidence of microvoid coalescence was observed as illustrated in Figure 7d. The high stress intensity levels caused failure of particles at greater distances from the overall crack plane. As a result, many more microvoids formed, and the fracture plane was microscopically rougher than it was at lower ΔK levels.

At the low and intermediate ΔK levels, the modified heat-treated welds exhibited fracture morphologies very similar to those observed in the conventional material. Below 19 MPa$\sqrt{m}$, corresponding to growth rate below 3×10^{-5} mm/cycle, slip offsets were observed on well-defined cleavage-like facets, shown in Figure 8. Under progressively higher ΔK conditions, up to 22 MPa$\sqrt{m}$, a transition from faceted growth to striation formation was detected. The entire fracture surface was covered with fatigue fissures, displayed in Figure 9a, with many fine striations lying between these secondary cracks. Figure 9b illustrates the typical well-defined fatigue striations that dominated the fracture surface at ΔK levels above 22 MPa$\sqrt{m}$.

The primary difference in fracture surface morphologies between the modified and conventional welds was the low density of microvoid coalescence in the former. This was expected because the modified treatment reduced the number

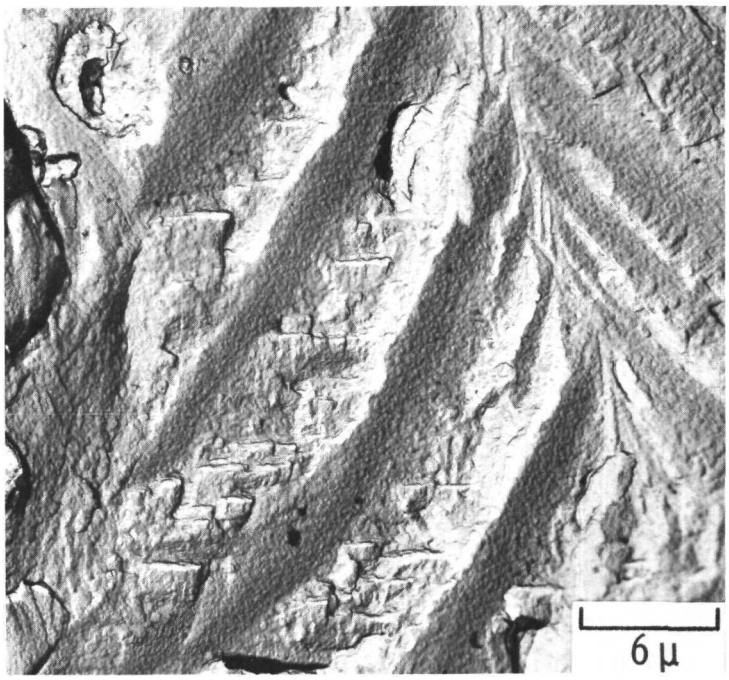

(a)

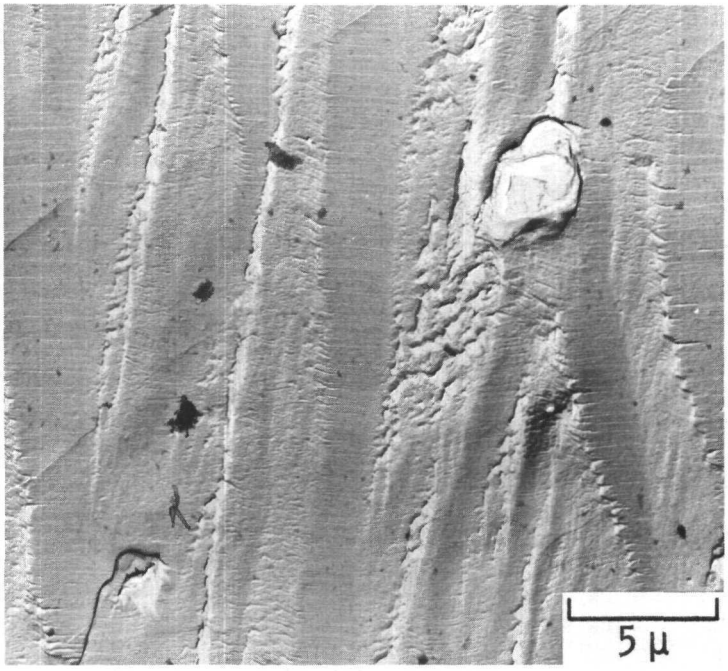

(b)

FIGURE 8. Electron Fractographs of Modified Weld at Low ΔK Levels.
(a) Crystallographic Facets.
(b) Slip Offsets on Facets.

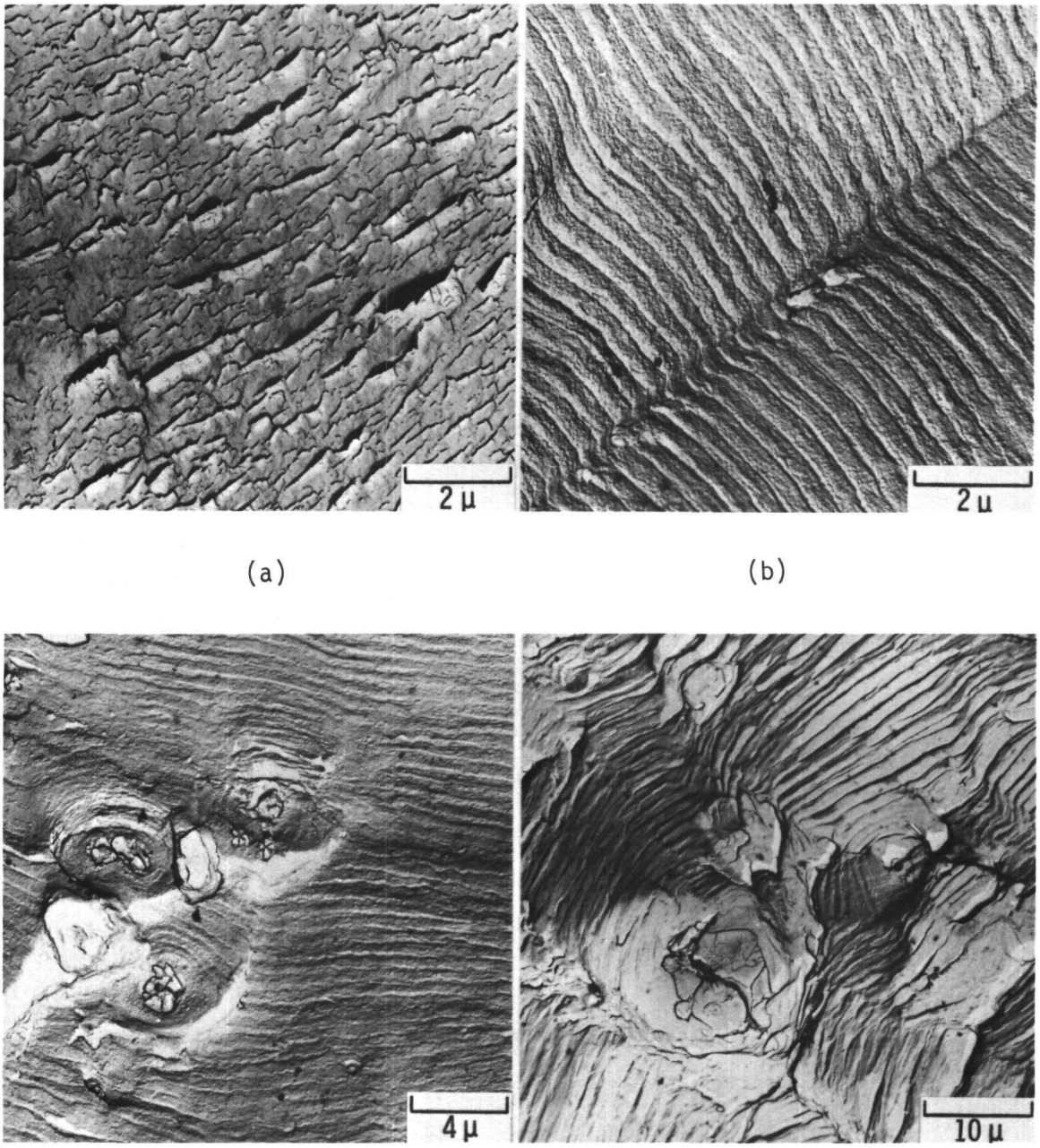

(a) (b)

(c) (d)

FIGURE 9. Fracture Surface Morphologies for the Modified Weld.
(a) Fatigue Fissures.
(b) Striations.
(c) Fatigue Striations Remaining Relatively Unaffected by the Presence of Dimples.
(d) Striation Morphology Affected Slightly by Microvoids.

(Neg. 8102955-4)

of nucleation sites by eliminating the δ phase and partially dissolving the Laves particles from the fusion zone. The few dimples found on the fracture surfaces (Figure 9c) did not appear to influence the microscopic fatigue behavior, since the orientation of adjacent striations was not altered significantly by their presence. At the highest growth rates, dimple rupture was more prominent (Figure 9d), but the density of dimples was still much lower than it was in the as-weld and conventional weldments. Striation morphology was affected slightly by these microvoids, indicating that the few remaining Laves particles exerted some influence on the overall fatigue response in the very high ΔK regime.

At temperatures up to and including 538°C, cracks propagated in a transgranular mode, and the operative fatigue mechanisms were found to be independent of test temperature. At 649°C, however, fracture surfaces exhibited extensive intergranular failure, as shown in Figure 10. In the conventional condition, some evidence of dimple rupture was observed, but the intergranular mechanism was dominant. The fracture surface of the modified heat-treated weld was completely intergranular.

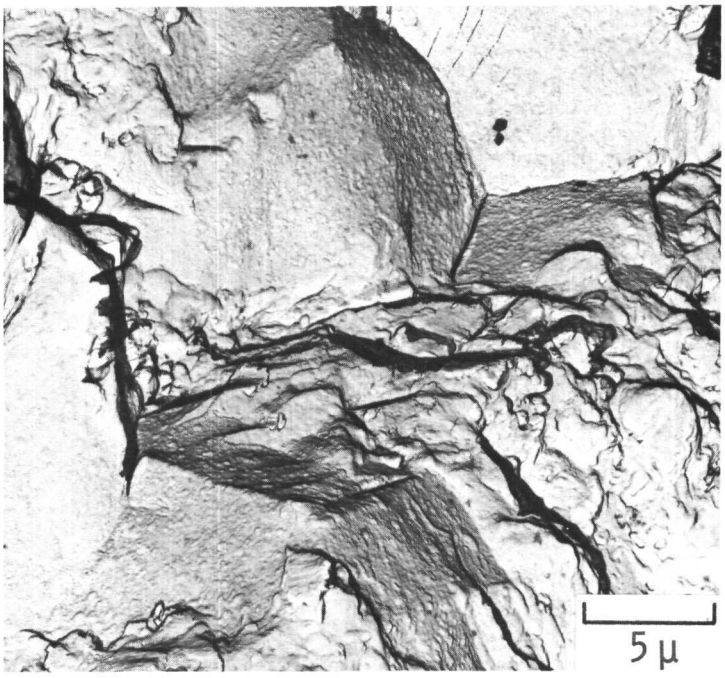

(a)

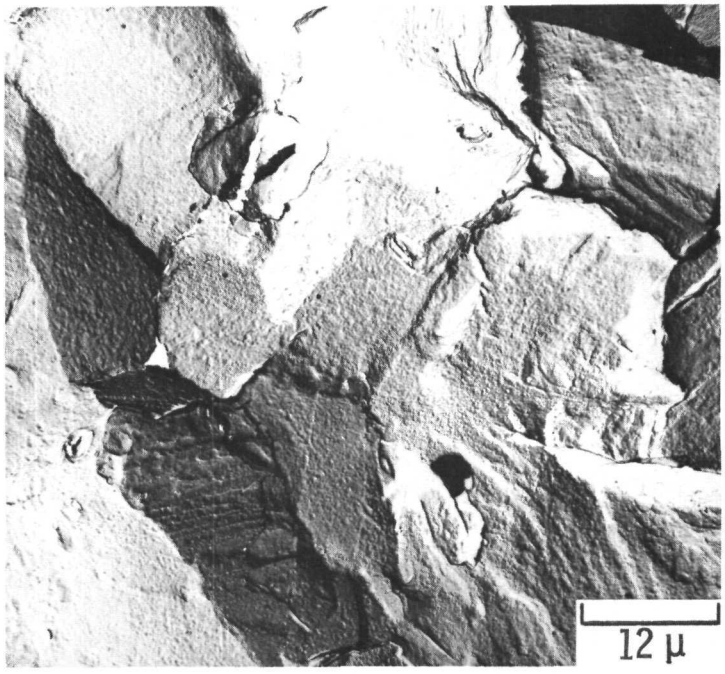

(b)

FIGURE 10. Typical Fracture Surface Appearance at 649°C.
(a) Conventional Weld Exhibiting Intergranular Failure with Some Evidence of Microvoid Coalescence.
(b) Modified Weld Displaying Only Intergranular Cracking.

DO NOT MICROFILM
THIS PAGE

IV. DISCUSSION

In this section, microscopic aspects of the fatigue behavior are correlated with macroscopic crack growth rates to explain the different responses exhibited by the as-welded, conventional and modified weldments. Striation spacing measurements provide quantitative information on microscopic growth behavior, so emphasis was placed on comparing striation spacings and macroscopic growth rates at 24 and 538°C where striation formation was dominant over a wide range of ΔK levels. These results are plotted on Figures 11 and 12 and compared with an empirical relationship proposed by Bates and Clark:[13]

$$\text{Striation Spacing} \approx 6\left(\frac{\Delta K}{E}\right)^2$$

where E is Young's modulus.

Considering first the cyclic response of the heat-treated welds, striation spacings were in agreement with the Bates and Clark prediction at room temperature, but fell slightly above the empirical relationship at 538°C. For a given striation spacing at this temperature, the Bates and Clark equation overestimates ΔK by approximately 20 to 40 percent. Figures 11 and 12 also reveal that microscopic growth rates in the modified weld were in agreement with macroscopic rates. In the conventional condition, striation spacings fell below the macroscopic curve with the discrepency increasing at the higher ΔK levels. Furthermore, striation spacing measurements for both heat treatments were essentially the same. Since microscopic growth rates for the conventional and modified welds were very similar, the difference in macroscopic growth rates at the higher ΔK levels was attributed to enhanced crack extension by the dimple rupture mechanism in the conventional weld. Hence, the Laves and δ particles, which nucleate microvoids in the weld zone under both monotonic[6] and cyclic loading conditions, result in the inferior fracture toughness and fatigue responses displayed by the conventional welds.

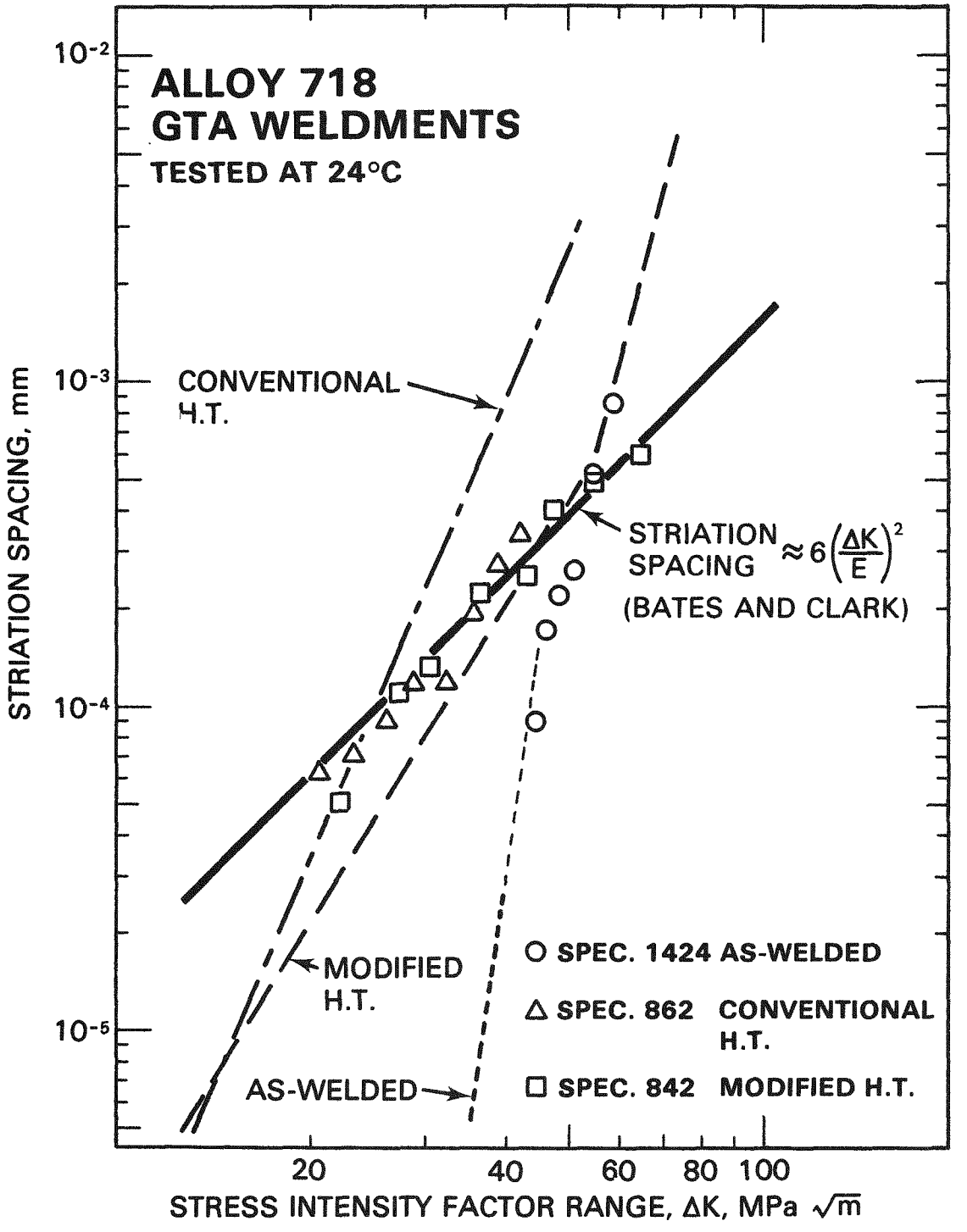

FIGURE 11. Comparison of Striation Spacings and Macroscopic Crack Growth Rates at Room Temperature. Each Data Point Represents an Average of Approximately 130 Striation Spacing Measurements.

(Neg. 8009381-1)

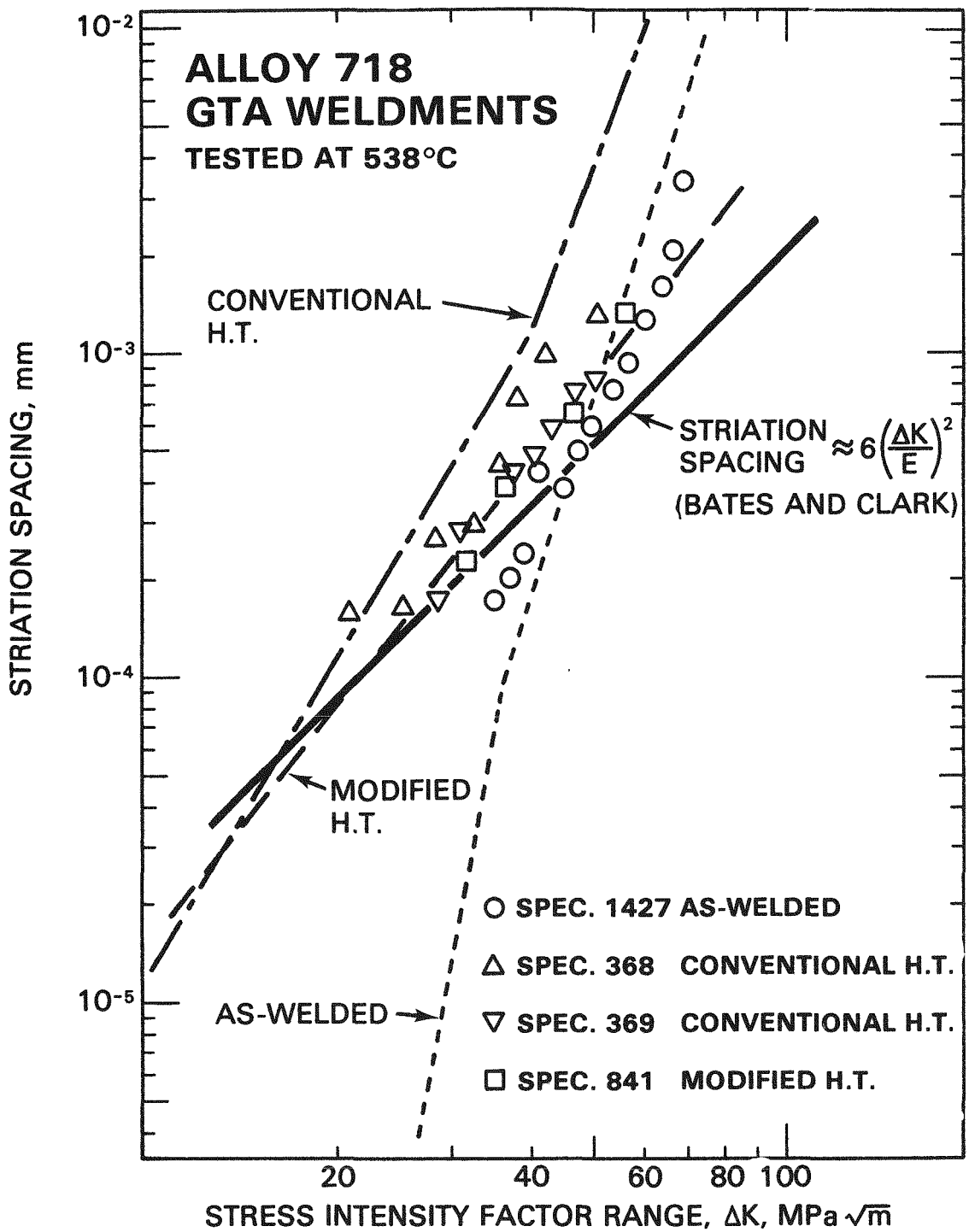

FIGURE 12. Comparison of Striation Spacings and Macroscopic Crack Growth Rates at 538°C. Each Data Point Represents an Average of Approximately 105 Striation Spacing Measurements.
(Neg. 8009381-2)

At ΔK levels below 20 MPa$\sqrt{m}$, the two heat treatments exhibited similar macroscopic growth rates. Since second phase particles did not interact with the advancing crack in this ΔK regime, the overall cyclic behavior for both the conventional and modified welds was controlled by the fatigue resistance of the similarly aged weld matrices (aging temperatures for both heat treatments were the same; only the solution annealing temperatures differed). Accordingly, both materials exhibited identical faceted growth mechanisms and comparable crack growth rates.

At 649°C the similar fatigue behavior exhibited by the conventional and modified welds, as shown in Figure 7 of Reference 1, is consistent with both heat treatments displaying intergranular fracture mechanisms. Moreover, the wrought metal also failed by an intergranular mechanism at this temperature, and its cyclic response was essentially the same as that of the welds.

The dramatic improvement in fatigue-crack propagation behavior for the as-welded condition was attributed to compressive residual stresses rather than metallurgical variables. Although the aged and unaged welds have rather different microstructures, these differences did not appear to explain the observed improvement in fatigue behavior. For example, metallurgical variables that could affect crack growth rates are the stacking fault energy and precipitate morphology of the weld matrix. In the as-welded condition, it can be argued that the absence of γ'' (body-centered-tetragonal Ni_3Nb) precipitates increases the Nb concentration in the matrix. This in turn lowers the stacking fault energy[14] in comparison to its aged counterpart, and lower stacking fault energies have generally been associated with superior fatigue resistance.[15] At 649°C, however, considerable precipitation of γ'' occurs within one hour.[16] The as-welded material, therefore, develops a microstructure and stacking fault energy comparable to those of the heat-treated welds early in the 649°C fatigue test. But crack growth rates at this temperature remain very low (Figure 7b in Reference 1), thereby indicating that stacking fault energy arguements cannot account for the improved fatigue behavior displayed by as-welded material.

Another possibility is that the Laves particles in the as-welded condition tend to impede the advancing fatigue crack at the low ΔK values. However, fatigue cracks in conventional welds also avoided second phase particles, but here no retardation of crack growth resulted. Consequently, it seems unlikely that such a retardation mechanism would operate in the as-welded condition.

The fact that the same fatigue mechanisms operate in the aged and unaged welds at comparable growth rates, but at rather different ΔK levels, suggests that the effective stress intensity range in the as-welded specimens may be very different from the applied stress intensity range. This idea is supported by the observation that Laves particles in the as-welded material remain intact at ΔK levels between 25 and 35 $MPa\sqrt{m}$, whereas in the conventional weld these particles failed and nucleated dimples at ΔK values above 20 $MPa\sqrt{m}$. These findings suggest that in the as-welded condition, compressive residual stresses introduced by the welding process significantly reduced the actual ΔK and K_{max} values as the crack tip. It has been shown[17-19] that such residual stresses can exert a profound influence on crack growth rates.

The typical residual stress distribution in the longitudinal welding direction, shown in Figure 13, is tensile in the center of the weldment, and is balanced by compressive stresses in the base plates. Bucci[19] proposed that this stress state sets up a clamping moment around the starter notch, which puts the crack tip in residual compression, as shown in Figure 13. This internal compressive force must be overcome by the applied load, thereby decreasing the cyclic stress intensity range effective in propagating the crack.

To determine if the clamping moment was present in the Alloy 718 weld, notches were machined into two specimen blanks, and the resulting front-face displacements were monitored at specific locations, in accordance with the procedure outlined by Bucci.[19] One specimen was tested in the as-welded condition; the second was annealed at 954°C. Displacements were measured

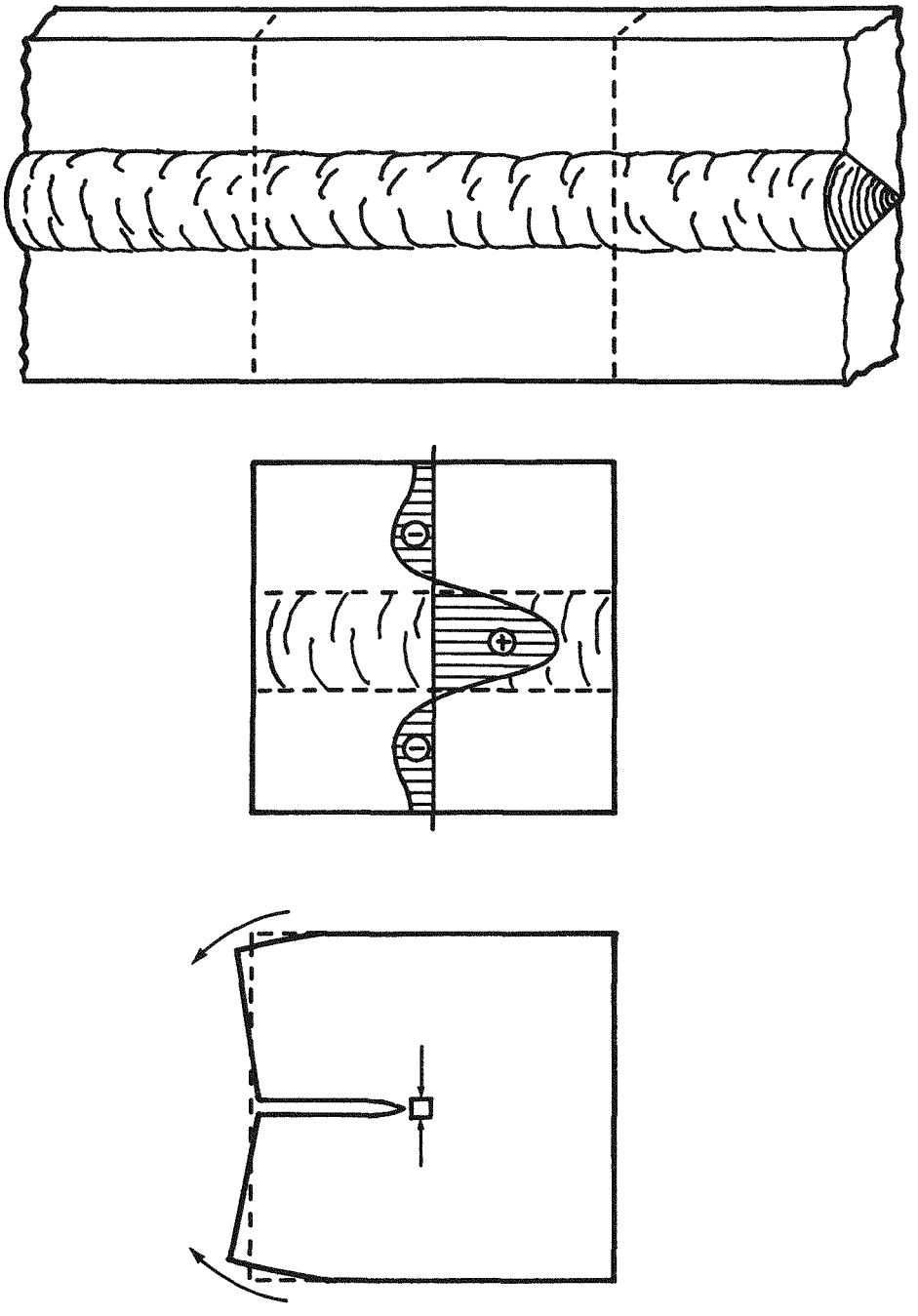

FIGURE 13. Typical Longitudinal Residual Stress Distribution in a Weld Compact Specimen and the Resulting Clamping Moment.[19]

at various locations on the front face after specimens were notched to depths of 13, 25 and 38 mm (Figure 14). The results are reported in Figures 15 and 16. In the as-welded condition, all displacements were toward the center of the weld indicating that clamping forces were definitely present. As the notch was progressively lengthened to simulate crack extension, the displacements continued to increase. Hence, significant residual stresses were present, at least at the shorter crack lengths simulated here.

Figure 15 also reveals that marks close to the center line moved more than those further away. This suggests that transverse internal stresses were also present and subsequently relieved by the introduction of the notch. These transverse forces can also influence crack growth rates. However, since transverse stresses are generally much lower than longitudinal stresses, it is believed that the internal clamping forces dominate. Finally, displacements near the top surface (crown) were slightly less than at the bottom, suggesting that there was a slight residual stress gradient through the thickness. Front-face displacements for the specimen annealed at 954°C prior to notching were found to be a factor of 5 smaller, as illustrated in Figure 16. Therefore, the solution anneals employed in the post-weld heat treatments removed the majority of internal forces.

It is concluded that the superior fatigue resistance of the as-welded material at low ΔK levels results from the presence of compressive residual stresses. In the higher ΔK regions, the as-welded crack growth rates approached those exhibited by the heat-treated welds for two reasons: the effects of the internal forces were overwhelmed by the large ΔK levels and the residual stresses were relieved at the longer crack lengths.

Figures 11 and 12 reveal that striation spacing measurements in the as-welded material were in agreement with macroscopic growth rates, but they deviated from the empirical Bates and Clark equation. The microscopic and macroscopic responses, however, do not represent the true material behavior because the internal forces altered the actual stress intensity at the crack tip. Since the operative fatigue mechanisms in the as-welded and

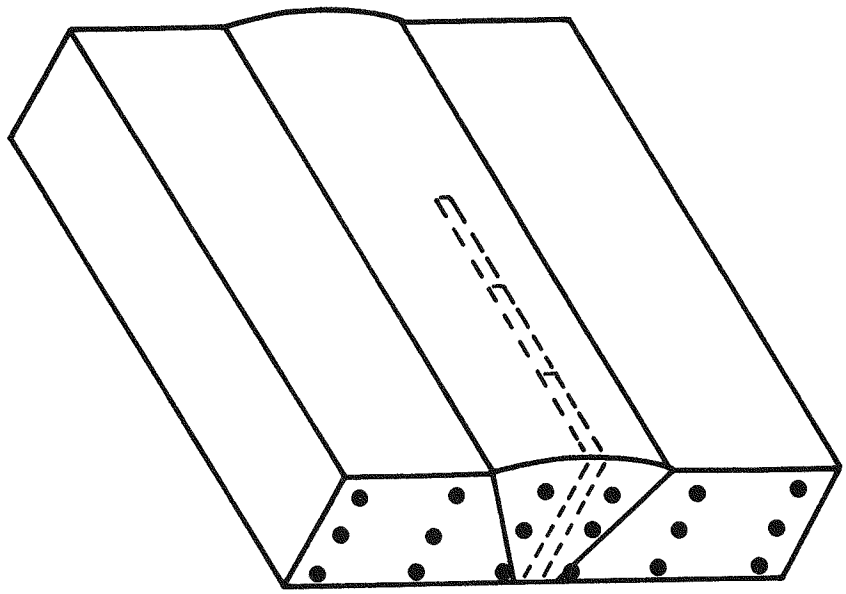

FIGURE 14. Notching of Specimen Blanks.

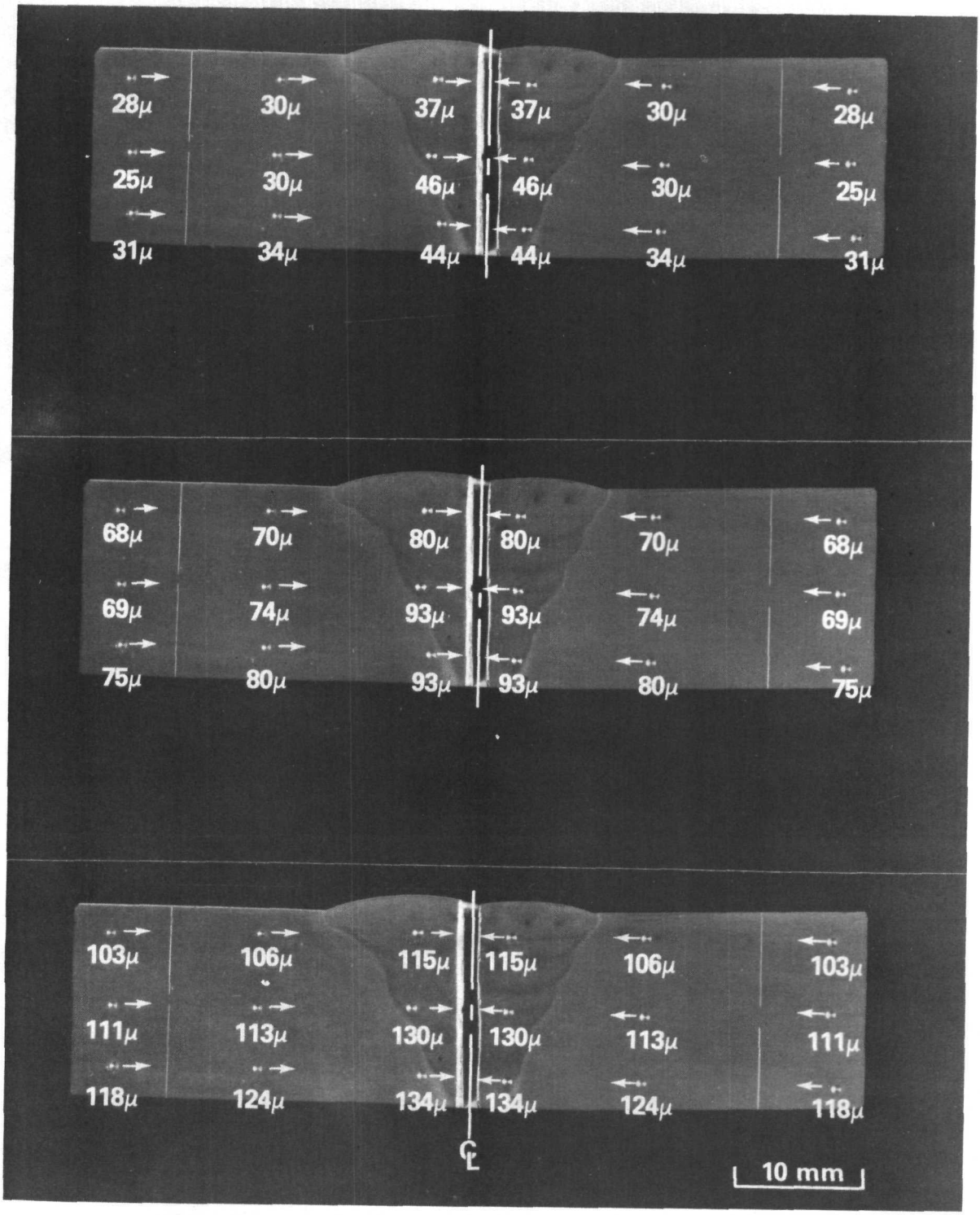

FIGURE 15. Front-Face Displacement in the As-Welded Specimen Blank After it was Notched. Displacement Given in μm. Notch Depths Were: (a) 13 mm; (b) 35 mm; and (c) 38 mm.

(Neg. 8102771-2)

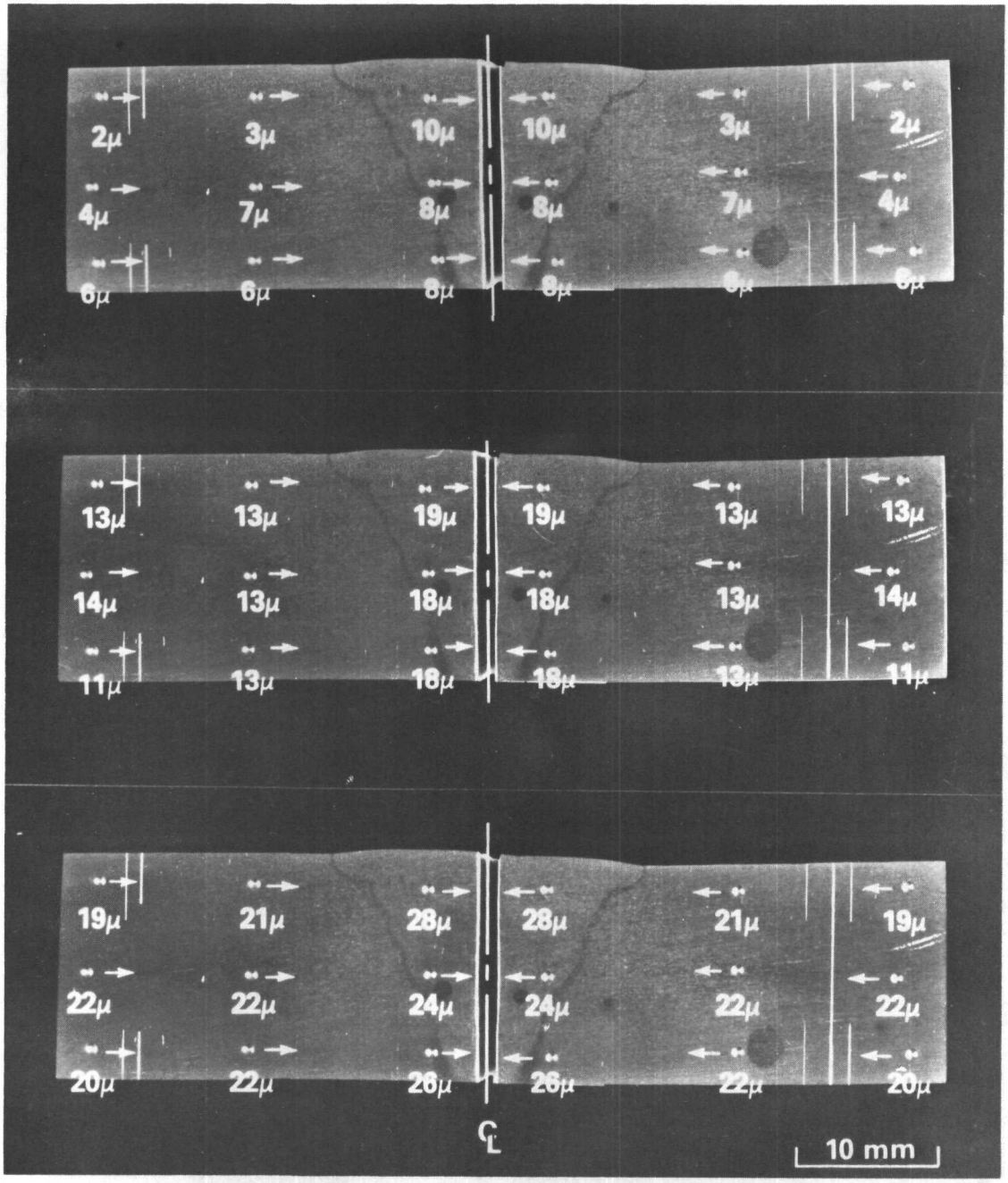

FIGURE 16. Front-Face Displacements in the Specimen Blank that was Annealed at 954°C. Displacements are given in μm. Notch Depths Were:
(a) 13 mm; (b) 35 mm; and (c) 38 mm.

(Neg. P10453-1)

DOE Richland, WA

conventional welds were very similar at equivalent growth rates, their true fatigue responses in the absence of residual stresses are probably very similar. In fact, at the higher ΔK levels where residual stress effects are minimal, as-welded and conventional heat-treated welds exhibited comparable crack growth rates (Figures 8 and 9 of Reference 1).

In summary, the presence of residual stresses in the as-welded condition had a dramatic influence on the microscopic and macroscopic fatigue behavior. As noted in the companion paper,[1] the residual stress distribution is affected by welding variables and component geometry. Therefore, the as-welded cyclic data reported in this and the companion papers are not true material properties; they only represent the fatigue response of a specific weldment.

DO NOT MICROFILM
THIS PAGE

V. CONCLUSIONS

Electron fractographic techniques were used to relate heat-treatment variations in the room and elevated temperature fatigue-crack growth behavior of Alloy 718 GTA weldments to operative fatigue mechanisms and key microstructural features. In general, fatigue fracture surface morphologies for the as-welded, conventional, and modified welds were found to be dependent on microstructure, temperature and effective stress intensity range as summarized below:

- The as-welded, conventional and modified welds all exhibited three basic fatigue mechanisms at temperatures up to 538°C: a cleavage-like faceted appearance at low crack growth rates, striation formation at intermediate rates, and microvoid coalescence coupled with coarse striations at very high growth rates. The major difference in fracture surface morphology was more pronounced dimple rupture in the as-welded and conventional weldments under intermediate and high ΔK conditions.

- Both the conventional and modified welds exhibited identical cleavage-like faceted growth mechanisms at low ΔK levels, which accounts for the similar crack growth rates displayed by the two heat treatments. In this regime, the second phase Laves and δ particles in the conventional material did not interact with the advancing crack. Therefore, the overall fatigue properties for both heat treatments were controlled by the fatigue resistance of the similarly aged matrices.

- Under progressively higher ΔK conditions, the inferior fatigue response exhibited by the conventional weld was attributed to Laves and δ particles nucleating extensive microvoid coalescence ahead of the advancing crack front. The largest difference in growth rates for the heat-treated welds occurred at high ΔK values where dimple rupture became the dominant fatigue mechanism in the conventional weld.

- At 649°C, the heat-treated Alloy 718 welds exhibited extensive intergranular failure and comparable crack growth rates.

- The dramatically improved fatigue resistance in the as-welded condition resulted from compressive residual stresses, which significantly reduced the effective ΔK and K_{max} values at the crack tip. Residual stresses also account for the aged and unaged welds exhibiting similar fracture surface morphologies under equivalent growth rates, but at very different ΔK levels. In the very high ΔK regime where residual stresses are much less important, crack growth rates in the as-welded and conventional welds were essentially the same.

- Since residual stresses have a profound effect on fatigue behavior, the microscopic and macroscopic crack propagation rates for the as-welded material reported in this and the companion paper are not true material properties.

- The high temperature solution anneal employed in the conventional and modified post-weld heat treatment relieved residual stresses within the weldment.

VI. REFERENCES

1. L. A. James and W. J. Mills, Effect of Heat Treatment Upon the Fatigue-Crack Growth Behavior of Alloy 718 Weldments - Part I: Macroscopic Behavior, HEDL-TME 81-12, Hanford Engineering Development Laboratory, Richland, WA, 1981.

2. J. C. Chesnutt and R. A. Spurling, "Fracture Topography Microstructure Correlations in the SEM", Metallurgical Transactions, Vol. 8A, pp. 216-218, 1977.

3. J. Gordine, "Some Problems in Welding Inconel 718", Welding Research Supplement, Vol. 50, pp. 480s-484s, 1971.

4. H. L. Eiselstein, "Metallurgy of Columbium-Hardened Nickel-Chromium-Iron Alloy", Advances in the Technology of Stainless Steel and Related Alloys, ASTM STP No. 369, pp. 62-77, 1963.

5. R. P. DeVries and G. R. Mamau, "Importance of a Relationship Between Dendrite Formation and Solidification in Highly Alloyed Materials", Journal of Metals, Vol. 20, No. 11, pp. 33-36.

6. W. J. Mills, Effect of Heat Treatment on the Elevated Temperature Tensile and Fracture Toughness Behavior of Alloy 718 Weldments, HEDL-TME 80-18, Hanford Engineering Development Laboratory, Richland, WA, May 1980.

7. M. J. Graber, C. R. Brinkman, R. R. Hobbins, Metallurgical Evaluation of Welding and Heat Treating Procedures for the Inconel 718 PBF In-Pile Tube, ANCR-1087, Aerojet Nuclear Company, Idaho Falls, 1975.

8. G. R. Smolik and W. G. Reuter, Heat Treatment Investigations for Welded Inconel 718 Pressure Vessels for the Power Burst Facility, ANCR-1227, Aerojet Nuclear Company, Idaho Falls, 1975.

9. W. G. Reuter, Design Data for the 1/4-in. Thick Alloy 718 In-Pile Tube, TREE-NUREG-1087, EG&G Idaho, Inc., Idaho Falls, 1977.

10. J. F. Barker, "A Superalloy for Medium Temperatures", Metal Progress, Vol. 81, pp. 72-76, 1962.

11. W. J. Mills and L. A. James, Effect of Heat-Treatment and Heat-To-Heat Variations in the Fatigue Crack Growth Response of Alloy 718 - Part II: Microscopic Observations, HEDL-TME 80-10, Hanford Engineering Development Laboratory, Richland, WA, April 1980.

12. C. D. Beachem, "Microscopic Fatigue Fracture Surface Features and the Influence of Propagation Angle Upon Their Formation", Transactions ASM, Vol. 60, pp. 324-343, 1967.

13. R. C. Bates and W. G. Clark, Jr., "Fractography and Fracture Mechanics", Transactions Quarterly, ASM, Vol. 62, pp. 380-389, 1969.

14. K. A. Hill, Microstructure and Joining of Ni-Ni_3Nb Unidirectionally Solidified Eutectic Composites, Master's Thesis, Lehigh University, 1973.

15. A. J. McEvily, Jr., and R. C. Boettner, "On Fatigue Crack Propagation in F.C.C. Metals", Acta Metallurgica, Vol. 11, pp. 725-743, 1963.

16. W. J. Mills, The Influence of Heat Treatment on the Microstructure and Mechanical Properties of Alloy 718 Base Metal and Weldments, HEDL-TME 78-54, Hanford Engineering Development Laboratory, Richland, WA, 1978.

17. L. A. James, "Fatigue-Crack Growth in Type 304 Stainless Steel Weldments at Elevated Temperatures", Journal of Testing and Evaluation, Vol. 1, No. 1, pp. 52-57, 1973.

18. B. M. Kapadia, "Influence of Residual Stresses on Fatigue Crack Propagation in Electroslag Welds", Fatigue Testing of Weldments, ASTM STP-648, pp. 244-260, 1978.

19. R. J. Bucci, Effect of Residual Stress on Fatigue Crack Growth Rate Measurement, presented at the 13th National Symposium on Fracture Mechanics, Philadelphia, PA, June 16, 1980.

DISTRIBUTION

UC-79 (122)

UC-79b (36)

UC-79h (27)

DOE/RRT-HQ (2)
Mail Stop B-107
Washington, DC 20545

Program Division Director

DOE/FFTFPO (5)

Director

HEDL (38)

TK Bierlein	W/A-1	B. Mastel	W/A-60
LD Blackburn	W/A-40	WJ Mills (2)	W/A-40
WF Brown	W/C-19	NF Panayotou	W/A-53
KW Carlson	W/A-40	WE Roake	W/C-16
DJ Criswell	W/A-40	CT Schaedel	W/A-46
DG Doran	W/A-57	LK Severud	W/C-98
AM Ermi	W/A-58	WF Sheely	W/A-62
DL Greenslade	W/A-40	JL Straalsund	W/A-61
GL Guthrie	W/C-39	WD Themar	W/A-40
GW Hollenberg	W/A-59	AL Ward	W/A-40
WL Hu	W/A-53	JA Williams	W/A-124
LA James (2)	W/A-40	GL Wire	W/A-58
GD Johnson	W/A-58	HH Yoshikawa	W/C-44
MD Jones	W/A-40	Central Files (5)	W/C-110
RL Knecht	W/A-40	Publ Services (2)	W/C-115
GC Massie	W/A-40		

DO NOT MICROFILM
THIS PAGE